Short-Time Dynamics Through Conical Intersections in Macrosystems

Lorenz S. Cederbaum,[1] Etienne Gindensperger,[1] and Irene Burghardt[2]

[1]*Theoretische Chemie, Universität Heidelberg, Im Neuenheimer Feld 229, D-69120 Heidelberg, Germany.*
[2]*Département de Chimie, Ecole Normale Supérieure, 24 rue Lhomond, F-75231 Paris cedex 05, France.*

The short-time dynamics through a conical intersection of a macrosystem with a vast number of nuclear degrees of freedom (modes) is investigated. For convenience, the macrosystem is decomposed into a system carrying a few modes and a "bath." By transforming the bath modes to new ones, it is shown that only three effective bath modes contribute to the conical intersection. They govern—together with the system's modes—the short-time dynamics of the macrosystem. The remaining bath modes do not directly couple the electronic states and become relevant at longer times. An extensive numerical example is presented.

By separating the electronic and nuclear motion, the Born-Oppenheimer approximation [1,2] enables us to picture electronic systems like molecules as a set of nuclei moving over a potential energy surface provided by the electrons. Whereas the validity of this basic approximation for the majority of chemistry, physics, and even biology is not in doubt, it is now clear that in many important cases the approximation breaks down. The nuclear and electronic motion then couple, and unexpected—so-called nonadiabatic—phenomena may arise. A particularly striking and important example of the result of the coupling between nuclei and electrons is a conical intersection between electronic states. A number of recent review articles and collections of articles on the subject amply demonstrate the existence and relevance of such intersections [3–8].

The nonadiabatic coupling matrix elements between electronic states are the largest possible at conical intersections where they become singular [3]. We may thus generally expect that such intersections give rise to the strongest possible nonadiabatic phenomena. Because of the extreme breakdown of the Born-Oppenheimer approximation, conical intersections provide pathways for ultrafast interstate crossing, typically on the femtosecond time scale. Conical intersections can be found already between low lying electronic states of triatomic molecules. Their abundance grows with increasing number of atoms in the system and with increasing density of electronic states. For truly large polyatomic molecules, conical intersections are ubiquitous.

The dynamics through conical intersections are inherently quantum mechanical in nature owing to the strong coupling between the nuclei and electrons. On the one hand, these dynamics are sensitive to the details of the Hamiltonian at the intersection and hence to the number of nuclear degrees of freedom (modes) involved. On the other hand, the effort to describe the quantum dynamics increases exponentially with the number of modes and inhibits the application to large systems. There has been a very promising development to compute multimode quantum dynamics (the multiconfiguration time-dependent

Hartree (MCTDH) algorithm [9,10]) which enables one to describe the motion of 20–30 degrees of freedom. Although substantial, this number is still small compared to the number of modes of the large systems we are interested in here.

In this work we investigate the possibility to study the quantum dynamics through a conical intersection in a macrosystem. By a macrosystem we mean either a large system like a macromolecule or a molecule embedded in an environment. Examples of an environment are a crystal or a protein pocket. The number of modes of the macrosystem is essentially infinite. We start with the linear coupling model Hamiltonian of the macrosystem with N_{MS} modes

$$H = -\Delta \boldsymbol{\sigma}_z + \sum_{i=1}^{N_{MS}} H_i; \qquad \boldsymbol{\sigma}_z = \begin{pmatrix} 1 & 0 \\ 0 & -1 \end{pmatrix} \quad (1)$$

where

$$H_i = \frac{\omega_i}{2}\left(p_i^2 + x_i^2\right)\mathbf{1} + \begin{pmatrix} \kappa_i^{(1)} x_i & \lambda_i x_i \\ \lambda_i x_i & \kappa_i^{(2)} x_i \end{pmatrix}. \quad (2)$$

The Hamiltonian (1) governs the nuclear motion of the modes with frequencies ω_i, coordinates x_i and canonical momenta p_i for two coupled electronic states vertically split by 2Δ. In Eq. (2), $\mathbf{1}$ is the unit matrix and the κ_i and λ_i denote the intrastate and interstate coupling constants. The linear coupling model reproduces correctly the adiabatic potential surfaces and the nonadiabatic couplings mentioned above in the vicinity of a conical intersection including, of course, the singularity of the latter [3,7,8]. The adiabatic surfaces are the potentials provided by the electrons and are usually obtained by electronic structure calculations. Here, they are given as the eigenvalues of H at frozen nuclei, i.e., at $p_i = 0$. The Hamiltonian (1) has been successfully used to compute the spectra and dynamics of many molecules [3,7,8].

We now decompose the Hamiltonian (1) into a "system" Hamiltonian H_S and a "bath" Hamiltonian H_B

$$H = H_S + H_B \qquad (3)$$

where $H_S = -\Delta\boldsymbol{\sigma}_z + \sum_{i=1}^{N_S} H_i$ and $H_B = \sum_{i=N_S+1}^{N_{MS}} H_i$.
The distinction between system modes and bath modes is
often arbitrary, but useful in general. In a case where our
macrosystem is a single large molecule, we may collect the
most relevant modes into H_S and all the remaining $N_B =
N_{MS} - N_S$ modes into H_B. If the macrosystem is a small
molecule embedded in an environment, the separation into
system and bath is obvious. We may, however, also shift
the most important bath modes, if available, into H_S. In
those, presumably rare cases where no relevant modes can
be identified whatsoever, we may even include all modes in
the bath, i.e., $N_S = 0$, $N_B = N_{MS}$.

The inclusion of H_B in any calculation presents a major
obstacle owing to the enormous number of modes in the
bath. In the following we shall introduce a unitary trans-
formation of the bath modes which decomposes H_B into a
computable part H_{eff} which, together with H_S, governs the
short-time dynamics of the macrosystem and a residual
part V_B which is relevant at longer times:

$$H_B = H_{\text{eff}} + V_B. \qquad (4)$$

Only three effective modes will be seen to span H_{eff}. It is
tempting to consider the elements $\sum_{i=N_S+1}^{N_{MS}} \kappa_i^{(\alpha)} x_i$, $\alpha = 1$,
2, and $\sum_{i=N_S+1}^{N_{MS}} \lambda_i x_i$ appearing in H_B as effective modes.
These modes are, however, neither orthogonal to each
other nor of physical relevance. To proceed, we notice
that these elements can be expressed as linear combina-
tions of three orthogonal modes. Two of them

$$X_{1,2} = \frac{1}{2K_{1,2}} \sum_{i=N_S+1}^{N_{MS}} \left(\frac{\kappa_i^{(1)}}{\bar{\kappa}^{(1)}} \pm \frac{\kappa_i^{(2)}}{\bar{\kappa}^{(2)}} \right) x_i \qquad (5)$$

determine the diagonal of H_{eff}. Here, $\bar{\kappa}^{(\alpha)} = [\sum(\kappa_i^{(\alpha)})^2]^{1/2}$
and $K_{1,2}$ are normalization constants ensuring that the sum
of the squares of the coefficients is unity. Obviously, the
vectors of coefficients of X_1 and X_2 in Eq. (5) are normal-
ized and orthogonal to each other. These coefficients de-
termine the first two columns of the unitary transformation
matrix T from the original coordinates $\vec{x} =
(x_{N_S+1}, \ldots, x_{N_{MS}})$ to the new ones $\vec{X} = (X_1, \ldots, X_{N_B})$: $\vec{X} =
\vec{x}T$. The third mode can be derived from the nondiagonal
element in H_B. By writing it as a linear combination of
three effective orthogonal modes, $\sum \lambda_i x_i = \Lambda_1 X_1 +
\Lambda_2 X_2 + \Lambda_3 X_3$, we readily obtain X_3 as well as the effective
coupling constants Λ_i, $i = 1 - 3$. This determines the
third column of T.

The knowledge of these three effective modes suffices to
derive the effective Hamiltonian envisaged in Eq. (4):

$$H_{\text{eff}} = \sum_{i=1}^{3} \frac{\Omega_i}{2}(P_i^2 + X_i^2)\mathbf{1}$$

$$+ \begin{pmatrix} \bar{\kappa}^{(1)}(K_1 X_1 + K_2 X_2) & \Lambda_1 X_1 + \Lambda_2 X_2 + \Lambda_3 X_3 \\ \Lambda_1 X_1 + \Lambda_2 X_2 + \Lambda_3 X_3 & \bar{\kappa}^{(2)}(K_1 X_1 - K_2 X_2) \end{pmatrix}$$

$$+ \sum_{i,j=1, j>i}^{3} d_{ij}\left(\frac{-\partial^2}{\partial X_i \partial X_j} + X_i X_j \right)\mathbf{1}. \qquad (6)$$

Clearly, only three modes contribute to H_{eff}. This
Hamiltonian consists of three terms of different physical
origin. The first one is just made of harmonic oscillators
with frequencies $\Omega_i = \sum_{j=N_S+1}^{N_{MS}} \omega_j t_{ji}^2$, where the t_{ij} are the
elements of the transformation matrix T. The second term
is responsible for the conical intersection and the coupling
between the electronic states, and the last term is a diago-
nal term in the electronic space. This term does not couple
the electronic states, it couples instead the three effective
modes. The respective coupling constants read: $d_{ij} =
\sum_{k=N_S+1}^{N_{MS}} \omega_k t_{ki} t_{kj}$.

All the remaining modes of the bath are, of course, in
V_B; see Eq. (4). Their definition now depends on the
remaining number $N_B - 3$ of columns of T. We can choose
this part of T in many ways as long as T is a unitary matrix.
A particular appealing choice gives

$$V_B = \sum_{i=4}^{N_B} \frac{\Omega_i}{2}(P_i^2 + X_i^2)\mathbf{1} + \sum_{i=1}^{3} \sum_{j=4}^{N_B} d_{ij}\left(\frac{-\partial^2}{\partial X_i \partial X_j} + X_i X_j \right)\mathbf{1}. \qquad (7)$$

Interestingly, V_B is diagonal in the electronic space and
does not couple the electronic states. V_B describes the
remaining $N_B - 3$ bath oscillators and how they couple
to the three effective modes spanning H_{eff}.

The decomposition of H_B into H_{eff} and V_B given above
is physically appealing. Only three modes play a direct role
in the coupling between the electronic states. As we shall
see below, this finding enables us to study accurately the
short-time dynamics through a conical intersection in a
macrosystem. Note that Yarkony has pointed out that the
linear terms of any conical intersection could be described
by three basic vectors [4,11]. These vectors are based upon
topological considerations and are distinct from, and com-
plementary to, the three effective modes introduced here
on the grounds of dynamical considerations.

To proceed we make contact with the autocorrelation
function [12,13] and with spectra which can be measured
in experiment. The autocorrelation function reads [3–7]

$$P(t) = \langle \overrightarrow{0} | e^{-iHt} | \overrightarrow{0} \rangle \qquad (8)$$

and describes the overlap of the wave functions at time t
and time 0 after excitation from the noninteracting elec-
tronic ground state to our manifold of coupled electronic
states. Since H is a matrix Hamiltonian in the present
context, $|\vec{0}\rangle$ is a column vector with elements $\tau_1|0\rangle$ and

$\tau_2|0\rangle$, where τ_1 and τ_2 are the transition matrix elements between the ground state and our two coupled electronic states. Depending on the experiment performed, $|\tau_\alpha|^2$ is the oscillator strength or ionization cross section for the state $\alpha = 1, 2$. The resulting spectra $P(E)$ are obtained by Fourier transformation of $P(t)$ [3–7,13]. The energy E is measured relative to the ground state energy.

The short-time dynamics is controlled by the first few cumulants [14]. Cumulants are obtained from the autocorrelation function; they are the coefficients of an expansion of $\ln[P(t)]$ about $t = 0$. Because of the intimate relationship between $P(t)$ and $P(E)$, cumulants are related to observable properties of the spectrum. The zeroth cumulant is the total intensity of the spectrum. In our case it is just $|\tau_1|^2 + |\tau_2|^2$ [obtained by setting $t = 0$ in Eq. (8)]. The first cumulant gives the center of gravity of the spectrum. The width of the spectrum is given by the second cumulant, and its major asymmetry by the third cumulant.

A major result of our effective modes analysis is that $H' = H_S + H_{\text{eff}}$ reproduces the zeroth, first, second, and third cumulants of the full Hamiltonian H exactly. In other words, if we calculate the dynamics using only the system's Hamiltonian and that of the three effective modes, we reproduce exactly the above mentioned properties of the spectrum. That the coupling term in V_B does not contribute to these cumulants can be easily seen if we express it by standard creation and annihilation operators instead of coordinates and momenta. A full account of the exact cumulants of H and those of H' is very lengthy and will be given elsewhere.

That H' reproduces the zeroth to third cumulants of H exactly is independent of the structure of H_S. Indeed, it is only required that the zeroth to third-order moments of H_{eff} vs H_B be identical. From a system-bath perspective, this further sheds light upon the system's evolution under a reduced propagator [15] whose effect on short time scales is determined by the first few *bath* moments in a cumulant expansion. The short-time—strongly non-Markovian—dynamics induced by this propagator can again be shown to be exactly described by H_{eff}. Details will be given elsewhere. Importantly, the conclusions of the present analysis hold for an arbitrary form of the system's Hamiltonian, beyond the linear coupling model of Eqs. (1) and (2).

The short-time dynamics through a conical intersection—as demonstrated above theoretically—is governed by a few modes only, those of the system and the three effective modes of the bath. This opens the way to study macrosystems. To test the performance of $H' = H_S + H_{\text{eff}}$ as compared to the full H, we need a numerically solvable example. Of course, such an example cannot include very many bath modes because the full H problem cannot be solved then. Fortunately, we can use the MCTDH method mentioned in the introduction to compute the dynamics of 20–30 modes. As our numerical example we choose butatriene in an "environment." For free butatriene it has been shown that two modes are dominant and reproduce the experimental spectrum well [16]. H_S consists of these two

modes. We describe the bath by 20 modes. Fifteen of them are so-called tuning modes and 5 are coupling modes. The frequencies, the intrastate and interstate coupling constants were chosen by a random number generator in the range $\omega_i \leq 0.40$ eV, $|\kappa_i^{(\alpha)}| \leq 0.13$ eV, and $|\lambda_i| \leq 0.22$ eV.

Four computations have been performed, all using MCTDH. (i) An exact calculation taking into account all the 22 modes of the "macrosystem." This calculation is already quite involved numerically. (ii) A calculation using the two modes of the system and the three effective modes. (iii) A calculation where the system's modes are considered as part of the bath, i.e., $N_S = 0$ and $N_B = 22$, and only three effective modes are used. (iv) A calculation of the system alone. In all these calculations the state $\alpha = 1$ has been populated by the excitation at time zero.

Figure 1(a) shows the autocorrelation function up to 40 fs for the four calculations listed above, which we briefly denote as the 22-mode, 2 + 3-mode, 0 + 3-mode,
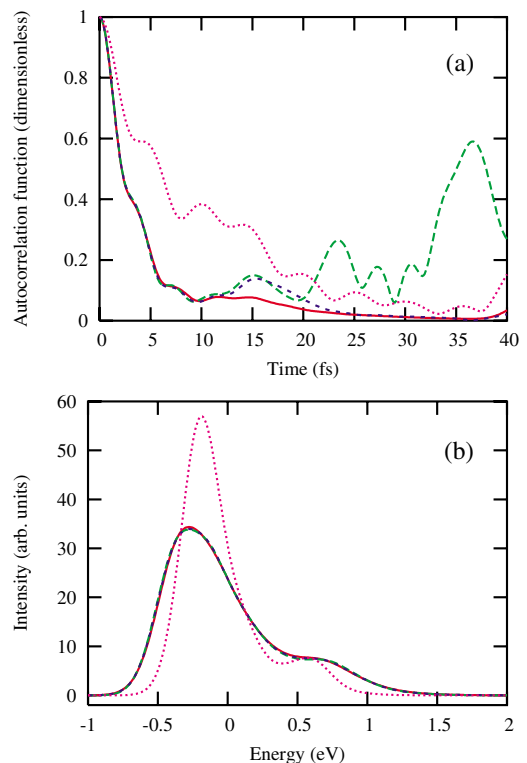
FIG. 1 (color online). (a) Autocorrelation function of butatriene coupled to a bath of 20 modes. The exact result and those of the effective modes are nearly indistinguishable up to 12 fs. (b) The corresponding band shape of the spectrum. The band shape is obtained by a Fourier transform of the autocorrelation function up to 200 fs, convoluted with a Gaussian of FWHM 0.13 eV. The exact result and those of the effective modes are nearly indistinguishable. Solid line (red online): exact result for the full system plus bath (22 modes). Dotted line (pink online): result for the system alone (2 modes). Dashed line (blue online): result for the system +3 effective modes for the bath. Long-dashed line (green online): result for the 3 effective modes defined to include the system plus bath.

and $2 + 0$-mode cases, respectively. If we compare the exact result to the one of the systems alone, we clearly see the huge effect of the bath: the autocorrelation function becomes smoother and decreases much faster and to a lower value. The two other curves correspond to the $2 + 3$-mode and $0 + 3$-mode results. For both we can see the excellent agreement with the exact one up to 12 fs. Then, some differences arise which are much stronger for the $0 + 3$-mode calculation. The $2 + 3$-mode result is roughly correct up to 40 fs, except for a ''bump'' between 13 and 22 fs. At longer times, i.e., after 40 fs (not shown), the differences become more substantial. The position of this bump in the autocorrelation function seems to correspond to the frequency of the most important effective mode, giving rise to a recurrence which also exists in the exact autocorrelation function but with lesser intensity. The short-time behavior of the $0 + 3$-mode result is also very good. At later times there is a clear deviation compared to the exact result. By including the system into the construction of the effective modes, we have further transferred the couplings into the remaining part V_B, which thus becomes more important. The direct influence of the system is ''drawn'' into the bath, and we observe at intermediate times strong recurrences due to the three effective modes. These features also exemplify that the contribution of the higher cumulants to the autocorrelation function is better reproduced at intermediate times if we separate the system from the bath. Nevertheless, the short-time dynamics is very well reproduced.

Importantly, the success of the effective-mode approach to reproduce the exact short-time dynamics implies that we can also well reproduce the band shape of the spectrum observed in low resolution experiments.

Figure 1(b) shows the band shapes as a function of energy for all four cases. Complete spectra are given by a Fourier transform of the autocorrelation function obtained from a long propagation in time. Their band shapes have been obtained by convoluting the spectra by a Gaussian of FWHM 0.13 eV. The width of the Gaussian is the only parameter we have to add, and we took the same value in the computation of all the band shapes. One sees that the band shape of the full problem is clearly different from the one of the system alone: different position and height of the maxima, different width, different asymmetry. As expected from the autocorrelation function, the results obtained with the effective-mode Hamiltonian are in very good agreement with the exact findings.

Let us conclude. We have studied the Hamiltonian of a macrosystem for a conical intersection situation. This Hamiltonian is formally decomposed into a system part H_S and a bath part H_B. While H_S can be of any structure, the linear coupling model is used for H_B which is known to reproduce correctly the dynamics in the vicinity of the conical intersection. A transformation of the bath modes to new ones leads to a natural decomposition of H_B into $H_{eff} + V_B$, where H_{eff} depends only on three effective modes. It is shown that the neglect of all other bath modes,

i.e., the use of $H' = H_S + H_{eff}$ as the Hamiltonian of the macrosystem, accurately reproduces the short-time dynamics of the macrosystem. Although the full Hamiltonian of the macrosystem may contain a vast number of modes, its short-time dynamics are governed by a few effective modes only. Since H' can be utilized with modern wavepacket propagation techniques (e.g., MCTDH), this opens the door to treat macrosystems in conical intersection situations. The effective-mode formulation very well reproduces the short-time dynamics and the band shape of a system coupled to a bath. However, to reproduce the autocorrelation function for longer times and the resolved spectrum of a macrosystem, one has to include the term V_B. Interestingly, V_B is a diagonal term in the electronic space and does not directly couple the two electronic states. It just bilinearly couples the three effective modes to the rest of the bath. We, therefore, expect that the impact of V_B on the dynamics can be well estimated using models for dissipation.

Finally, we mention that the present theory can easily be extended to the situation where more than two electronic states couple. For n coupled states the number of effective modes should be $n(n + 1)/2$.

---

[1] M. Born and R. Oppenheimer, Ann. Phys. (Berlin) **84**, 457 (1927).

[2] M. Born and K. Huang, *The Dynamical Theory of Crystal Lattices*, (Oxford University Press, Oxford, UK, 1954).

[3] H. Köppel *et al.*, Adv. Chem. Phys., **57**, 59 (1984).

[4] D. R. Yarkony, Rev. Mod. Phys. **68**, 985 (1996).

[5] M. A. Robb *et al.*, in *Reviews in Computational Chemistry*, edited by K. Lipkowitz and D. Boyd (Wiley, New York, 2000), vol. 15, p. 87.

[6] *The Role of Degenerate States in Chemistry*, edited by M. Baer and G. D. Billing, Advances in Chemical Physics Vol. 124 (Wiley, Hoboken, 2002).

[7] *Conical Intersections: Electronic structure, Dynamics and Spectroscopy*, edited by W. Domcke, D. R. Yarkony, and H. Köppel (World Science, Singapore, 2004).

[8] G. A. Worth and L. S. Cederbaum, Annu. Rev. Phys. Chem. **55**, 127 (2004).

[9] H. D. Meyer *et al.*, Chem. Phys. Lett. **165**, 73 (1990).

[10] M. H. Beck *et al.*, Phys. Rep. **324**, 1 (2000); G. A. Worth *et al.*, The MCTDH Package, Version 8.2, 2000; H.-D. Meyer, The MCTDH Package, Version 8.3, 2002; see http://www.pci.uni-heidelberg.de/tc/usr/mctdh/.

[11] D. R. Yarkony, Acc. Chem. Res. **31**, 511 (1998).

[12] R. D. Levine, *Quantum Mechanics of Molecular Rate Processes* (Oxford University Press, New York, 1969).

[13] E. J. Heller, J. Chem. Phys. **68**, 2066 (1978).

[14] H. Cramér, *Mathematical Methods of Statistics* (Princeton University Press, Princeton, 1946).

[15] A. Royer, Phys. Rev. Lett. **77**, 3272 (1996).

[16] C. Cattarius *et al.*, J. Chem. Phys. **115**, 2088 (2001).